Low temperature electron paramagnetic resonance anomalies in Fe-based nanoparticles

Yu. A. Koksharov
Faculty of Physics, M.V. Lomonosov Moscow State University, Moscow, Russia

S. P. Gubin
N.S. Kurnakov Institute of General and Inorganic Chemistry, Moscow, Russia

I. D. Kosobudsky
Chemical Department, Saratov State University, Russia

M. Beltran and Y. Khodorkovsky[a)]
Beltran, Incorporated, 1133 East 35th Street, Brooklyn, New York 11210

A. M. Tishin
Faculty of Physics, M.V. Lomonosov Moscow State University, Moscow, Russia and Beltran, Incorporated, 1133 East 35th Street, Brooklyn, New York 11210

(Received 6 October 1999; accepted for publication 22 March 2000)

A study of the electron paramagnetic resonance of Fe-based nanoparticles embedded in polyethylene matrix was performed as a function of temperature ranging from 3.5 to 500 K. Nanoparticles with a narrow size distribution were prepared by the high-velocity thermodestruction of iron-containing compounds. A temperature-driven transition from superparamagnetic to ferromagnetic resonance was observed for samples with different Fe content. The unusual behavior of the spectra at about 25 K is considered evidence of a spin-glass state in iron oxide nanoparticles. © *2000 American Institute of Physics.* [S0021-8979(00)01213-5]

I. INTRODUCTION

The field of nanoscale systems is important for fundamental physics as well as for many new technologies. Nanometer-sized structures are an intermediate form of matter that fills the gap between atoms/molecules and bulk materials. These types of structures often exhibit exotic physical and chemical properties different from those observed in bulk three-dimensional materials.

The recent advances in magnetic recording have made it necessary to improve the capacity of magneto-optical storage and recording heads using giant magnetic resistivity effects. At the same time, there is presently a need for the development of high-density retrieval data storage systems that can operate under such hazardous environmental conditions as high and low temperature, mechanical shock, and humidity. A real advance in this direction is the creation of new functional matrices and the use of novel principles for the fabrication of nanosized incorporated elements. One of the possible ways of progressing in the field of high density data storage systems is to utilize magnetic nanoparticles. As an example, this material could contain single domain nanoparticles uniformly distributed in a polymer matrix.

Magnetic nanoparticles embedded in different nonmagnetic matrices have been the subject of intense current research.[1,2] It is well known[3] that at sufficiently high temperatures noninteracting single-domain magnetic particles show superparamagnetic properties that can be characterized by the relaxation time τ_R. The relaxation time depends on temperature as $\tau_R = \tau_0 \exp(KV/k_BT)$, where K is the magnetic anisotropy constant, V is the particle volume, and τ_0 is on the order of 10^{-10}–10^{-12} s.[4] Below the blocking temperature T_B, which depends on a typical time scale of measurements τ, these particles undergo a transition to a so-called stable state.[3] At the blocking temperature the relation $\tau_R \approx \tau$ is satisfied. The most commonly used techniques for the determination of T_B are Mössbauer spectroscopy and magnetization measurements.[5] In Mössbauer experiments the magnetic hyperfine splitting disappears above the temperature T_B^M, at which $\tau_R \approx 5 \times 10^{-9}$ s.[4] It is widely accepted that we can determine the value of the magnetic blocking temperature T_B^m as the position of the maximum on the zero-field-cooled curves of magnetization, at which $\tau_R \approx 10^2$ s.[3,6] The study of the ratio T_B^M/T_B^m for different nanoparticle systems is very important since it allows one to arrive at conclusions with respect to interparticle interaction effects.[4]

Electron paramagnetic resonance (EPR) spectroscopy is recognized as a powerful research method for different bulk magnetic materials including ferro- and antiferromagnets and spin-glasses.[7,8] The transition to the magnetic ordered state can be easily detected by the EPR method.[7] The linewidth, the resonance field, and the intensity of the EPR line usually show distinct abnormal behavior near the transition temperatures.[7,8] For nanoparticle systems (NPSs) an analog of the magnetically ordered state is the stable state. As a rule, some peculiarities in EPR spectra should be observed near the blocking temperature. What, however, is the characteristic temperature for EPR in NPS that is similar to T_B^M and T_B^m

[a)]Author to whom correspondence should be addressed; present address: Beltran, Inc., 1133 East 35th Street, Brooklyn, NY 11210; electronic mail: beltran@earthlink.com

for Mössbauer spectroscopy and magnetization measurements?

The microwave properties of different NPS were investigated both experimentally[9–22] and theoretically.[19–27] Most of these works were limited to room temperature measurements. The thermal behavior of EPR spectra observed in ferrofluids[12,13,15] and precipitates in glasses[20] cannot be interpreted adequately within the models developed in the last years.[20,23–26] In this connection, any new experimental data concerned with the temperature features of EPR in NPS seem to be important.

In this article we present a detailed EPR study of Fe-based nanoparticles embedded in polyethylene matrix. It is well known that nanoparticles are thermodynamically unstable. For their stabilization we have used the polyethylene (PE). This polymer is relatively resistant to heat and oxidation and is chemically inert. PE is a typical semicrystalline polymer with a degree of crystallinity usually lying within a range between 60% and 80%. Both the crystal and, particularly, the amorphous parts of polymers contain a significant number of vacancies. The nanoparticles grow inside these vacancies during the thermodestruction of iron-containing compounds (ICCs). Samples with different Fe content (from 1–50 wt %) were prepared. In samples with a high iron concentration, interparticle interactions can be significant. Our measurements showed that EPR spectra are very sensitive to the Fe content. In this article EPR data are presented for samples with relatively low Fe contents of 1 and 5 wt % (samples S1 and S5, correspondingly). It is assumed that in these samples the interactions between particles should be minimal.

II. EXPERIMENTAL PROCEDURE

The samples were obtained by the high-speed thermal decomposition of ICC in a solution/melt of polyethylene in vaseline oil in an inert atmosphere at 220 °C. The microwave absorption was measured using an *X* band (~9.2 GHz) EPR spectrometer E-109 (''Varian'', USA). Magnetic fields up to 5 kOe were provided by a Varian Associates 12 in. electromagnet. A standard field modulation (100 kHz) and phase-sensitive detector techniques were used, so that the detected signal corresponded to the field derivative of the absorbed power. Two principal characteristics of EPR were calculated from the spectra: the resonance field H_R and the linewidth of the resonance $\Delta H_{\rm pp}$ (peak-to-peak). The resonance field H_R was defined as the field for a middle point of the spectrum between maximum and minimum peaks. The resonance field complements the effective g value, defined by the relation $g_{\rm eff}=2H_e/H_R$, where H_e is the resonance field corresponding to a free-spin marker like diphenylpicrylhydrazyl. The signal amplitude (the difference between absolute maximum and minimum) was also analyzed.

The microwave absorption signal was recorded with the modulation field amplitude of 10 Oe at the microwave power 10 mW. A specially made test shows that at room temperature the EPR signals are proportional to the microwave power up to 200 mW with no sign of saturation. The temperature was controlled by a flow helium cryostat system (Oxford Instruments, USA) from 4.2 to about 300 K as well as a nitrogen variable temperature system E-257 (Varian) from 120 to about 500 K. In our low temperature experiments the samples were cooled down to 4 K in a remanent field (100 Oe) of the magnet, then the samples were heated and the EPR spectra were recorded at different temperatures.

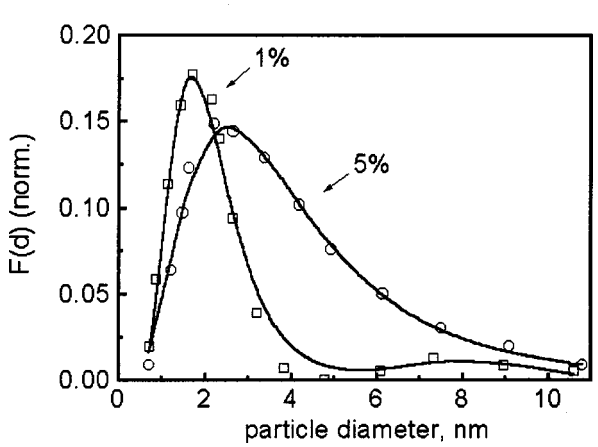

FIG. 1. Particle size distributions for samples S1 and S5. $F(d)$ is the normalized probability to find a nanoparticle with a diameter which is equal to d. Solid lines correspond to the best fit of the experimental data by using log-normal distribution. Squares (sample S1) and circles (sample S5) represent experimental data.

III. EXPERIMENTAL RESULTS

The samples were characterized by the x-ray Fe $K_{\beta 5}$ emission and Mössbauer spectroscopy methods as well as by small angle x-ray scattering (SAXS) analysis. According to the data of the x-ray emission and the Mössbauer spectroscopy, more than 80% of nanoparticle mass is formed by iron oxide ($\gamma-Fe_2O_3$). The x-ray emission $K_{\beta 5}$ spectra also indicated that bonds ($Fe–O–CH_2$, $FeOH–CH_2OH$ etc.) can be formed between the iron atoms on the nanoparticle surface and the surrounding matrix typical of metalorganic compounds.

The results of the SAXS study are shown in Fig. 1. For sample S1, the nanoparticle size distribution is close to bimodal log-normal[28,29]

$$F(d)=A_1/(2\pi\sigma_1^2)^{1/2}\exp[-\ln^2(d/d_{m1})/2\sigma_1^2] + A_2/(2\pi\sigma_2^2)^{1/2}\exp[-\ln^2(d/d_{m2})/2\sigma_2^2],$$

where

$$A_1=0.023\pm0.001,\quad d_{m1}=20.0\pm0.4,$$

$$\sigma_1=0.17\pm0.01,$$

$$A_2=0.0008\pm0.0005,\quad d_{m2}=82\pm12,$$

$$\sigma_2=0.08\pm0.07.$$

For sample S5, the nanoparticle size distribution is log-normal

$$F(d)=A/(2\pi\sigma_1^2)^{1/2}\exp[-\ln^2(d/d_m)/2\sigma^2],$$

where

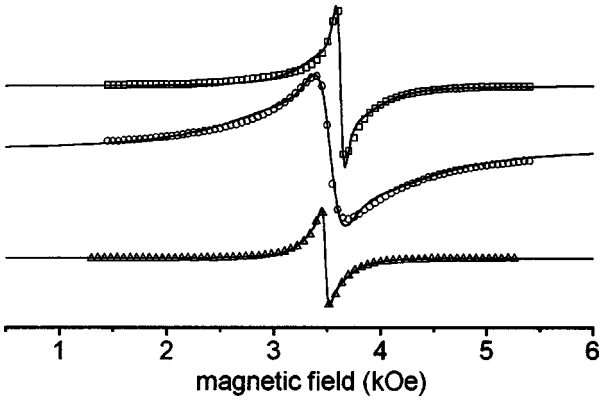

FIG. 2. EPR spectra of samples S1 and S5. Experimental data are represented by squares (sample S1 at 300 K), circles (sample S5 at 300 K), and triangles (sample S5 at 500 K). Solid lines show results of the numerical fitting to Lorentzian line shape.

$$A = 0.0255 \pm 0.0004, \quad d_m = 35.7 \pm 0.4,$$

$$\sigma_1 = 0.171 \pm 0.007.$$

The room temperature EPR spectra of samples S1 and S5 are shown in Fig. 2. The observed resonance lines cannot be fitted by a single Lorentzian or Gaussian curve. The strongest and relatively narrowest ($\Delta H_{pp} \approx 150$ Oe) signal was fitted by the sum of two Lorentzian lines

$$f(H) = B_1(H-H_1)/\{(H-H_1)^2 + \Delta H_1^2\} + B_2(H-H_2)/\{(H-H_2)^2 + \Delta H_2^2\}.$$

The lines in Fig. 2 present the results of fitting, providing the following parameters for samples S1 and S5 at different temperatures:

(a) $B_1/B_2 = 0.023$, $H_1 = (3621 \pm 1)$ Oe, $\Delta H_1 = (138 \pm 1)$ Oe, $H_2 = (3619 \pm 1)$ Oe, $\Delta H_2 = (690 \pm 5)$ Oe, (S1, 300 K);

(b) $B_1/B_2 = 0.026$, $H_1 = (3524 \pm 1)$ Oe, $\Delta H_1 = (440 \pm 7)$ Oe, $H_2 = (3515 \pm 4)$ Oe, $\Delta H_2 = (1820 \pm 10)$ Oe, (S5, 300 K);

(c) $B_1/B_2 = 0.034$, $H_1 = (3481 \pm 1)$ Oe, $\Delta H_1 = (114 \pm 1)$ Oe, $H_2 = (3486 \pm 1)$ Oe, $\Delta H_2 = (417 \pm 2)$ Oe, (S5, 500 K).

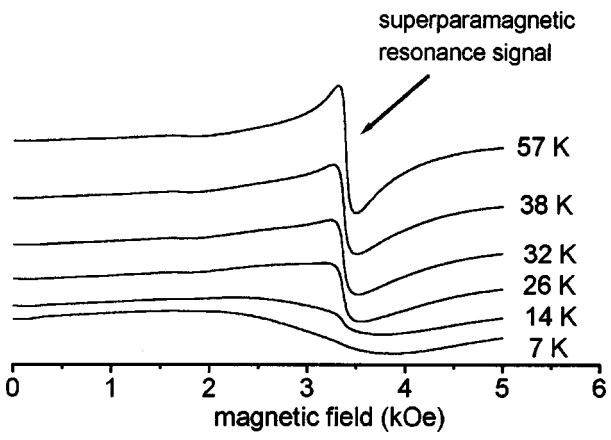

FIG. 3. EPR spectra of sample S1 at low temperatures.

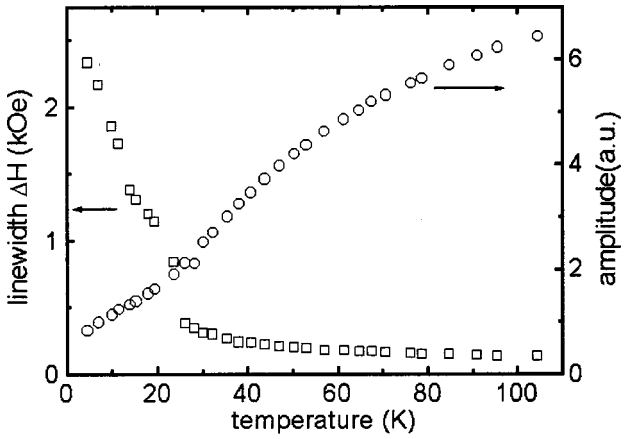

FIG. 4. Thermal variations of the EPR linewidth and signal amplitude for sample S1.

Figure 3 shows the spectra of sample S1 at low temperatures. Down to about 30 K an intensive line with $g_{eff} \approx 2.0$ dominates in the spectra. In addition, a small feature is visible at about 1700 Oe ($g \approx 3.8$). As the temperature decreases, a broad ($\Delta H_{pp} > 1$ kOe) line grows and becomes prevalent below approximately 20 K.

The thermal variations of the ΔH_{pp} and EPR signal amplitude A are presented in Fig. 4. It is evident from Fig. 4 that near 25 K, the spectrum changes drastically. The relatively narrow line disappears and is replaced by the broad one. This spectrum transformation is presented in more detail in Fig. 5. In all the studied temperature ranges both narrow and broad lines demonstrate a decrease of the amplitude and a broadening under sample cooling. The spectrum breadth is especially evident below 25 K (Fig. 4).

The thermal behavior of the EPR spectra of sample S5 resembles that of sample S1. A distinction consists of the shift of all characteristic temperatures to higher values. For example, the room temperature spectra of samples S1 and S5 are very different (Fig. 2). However, the EPR spectrum of sample S5 at 500 K is much more similar to the room temperature spectra of sample S1 (Fig. 2). This tendency also

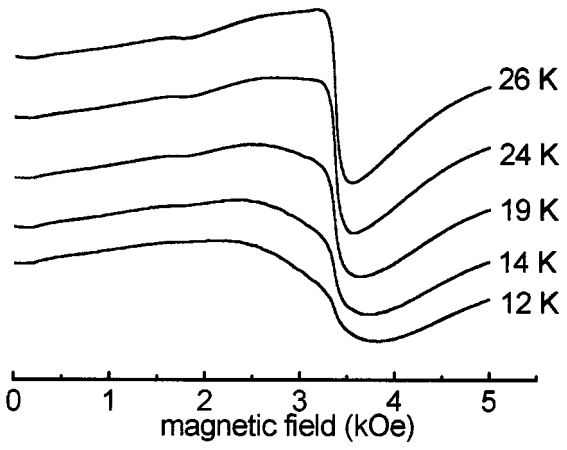

FIG. 5. The transformation of EPR spectra of sample S1 below 25 K.

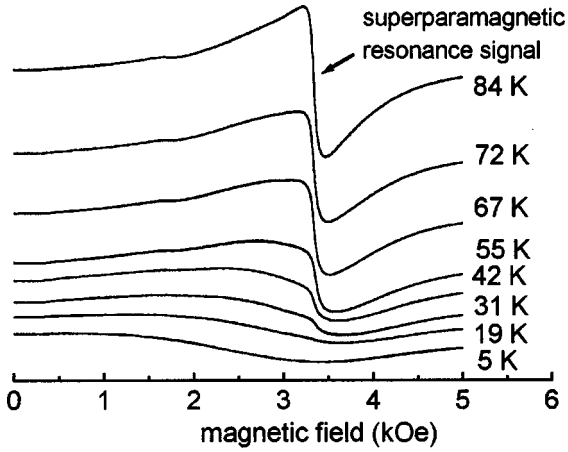

FIG. 6. EPR spectra of sample S5 at low temperatures.

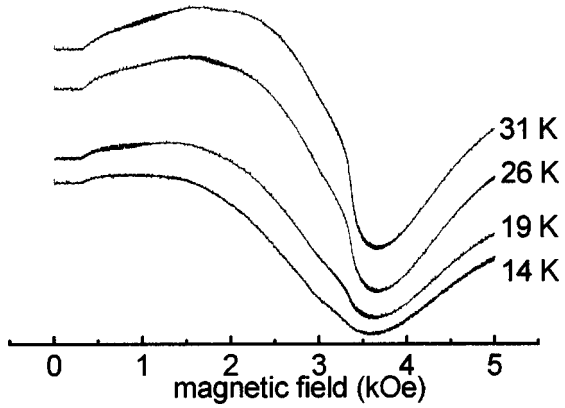

FIG. 8. EPR spectra of sample S5 below 30 K.

takes place at low temperatures (Figs. 3 and 6). Figure 6 shows the EPR spectra of sample S5 below 85 K. It is apparent that the broad line becomes dominant in the spectra near 70 K (Fig. 6). The thermal variations of the EPR linewidth and signal amplitude of sample S5 are presented in Fig. 7. It is interesting that for sample S5 a marked spreading of the EPR line is observed near 25 K (Fig. 8) in the same way as for sample S1 (Fig. 5).[30]

IV. DISCUSSION

The nanoparticles in the samples studied are subject to three kinds of interactions: (a) with the matrix; (b) with other particles; and (c) with the applied magnetic field. The support, or matrix, within which nanoparticles are synthesized, plays an active role in determining their physical properties. It is necessary to note that interaction (b) strongly depends on the nature (conductivity) of the matrix as well as on the interparticle distance and distribution within the matrix. The advantages of polymer matrices are associated with a relative chemical inertness and reasonably narrow particle size distribution.[31] We assume that interactions with the diamagnetic PE matrix have no direct effect on the resonance phenomenon. However, the solid matrix keeps the particles in place, so that they cannot rotate in the applied external magnetic field. This sets polymer matrices apart from ferrofluids.

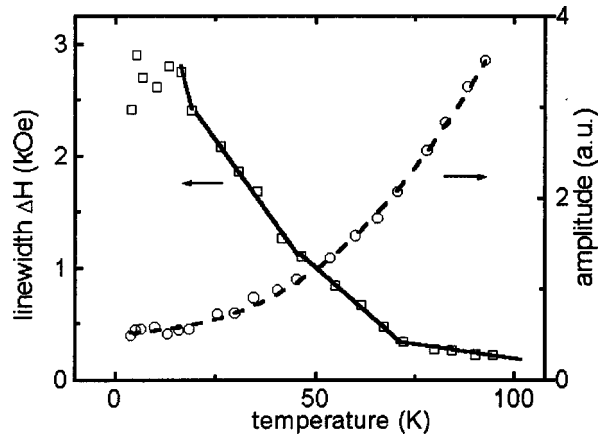

FIG. 7. Thermal variations of the EPR linewidth and signal amplitude for sample S5.

The magnetic properties of NPS are sensitive not only to particle size but also to the average interparticle distance. If the latter reaches some critical value, spin-glass-like ordering could take place.[32,33] Since in a dielectric matrix magnetic nanoparticles interact only by dipolar interactions, the temperature of the collective transition has to qualitatively obey the $(1/a)^3$ law where a is the average interparticle distance. The relationship the between Fe concentration and a may be obtained by the following analysis.

Let η_m stands for the weight concentration of Fe in a polyethylene matrix. Then the volume concentration η_V can be expressed as

$$\eta_V = V_{\mathrm{Fe}}/V_{\mathrm{PE}} = (m_{\mathrm{Fe}}/m_{\mathrm{PE}})(\rho_{\mathrm{PE}}/\rho_{\mathrm{Fe}}) \approx \eta_m(1\ \mathrm{g\,cm^{-3}}/4.8\ \mathrm{g\,cm^{-3}}) = 0.2\ \eta_m, \tag{1}$$

where $V_{\mathrm{Fe}}(V_{\mathrm{PE}})$ and $m_{\mathrm{Fe}}(m_{\mathrm{PE}})$ are the volume and the mass of the ferrous (polymer) part of the sample, and ρ_{PE} and ρ_{Fe} are the densities of the polyethylene and iron oxide, correspondingly.

Let us assume that a studied sample is cube shaped, the length of the edge is equal to L, and each nanoparticle is a sphere with radius R. Let us also suppose that the particles are uniformly distributed in the polymer matrix. It is obvious that the number of particles in the sample is equal to $N = (L/a)^3$. The volume of Fe in the sample can be expressed as

$$V_{\mathrm{Fe}} = N(4\pi R^3)/3 = N(\pi d^3)/6 = (L/a)^3 v = (V_{\mathrm{PE}} + V_{\mathrm{FE}})(v/a^3),$$
$$a^3/v = 1 + V_{\mathrm{PE}}/V_{\mathrm{FE}} = 1 + 5/\eta_m, \tag{2}$$

where v and d are the nanoparticle volume and diameter, correspondingly.

Using Eqs. (1) and (2) we obtain

$$a^3 = (1 + 5/\eta_m)(\pi d^3)/6,$$
$$a \approx [(\pi/6)(1 + 5/\eta_m)]^{1/3} d. \tag{3}$$

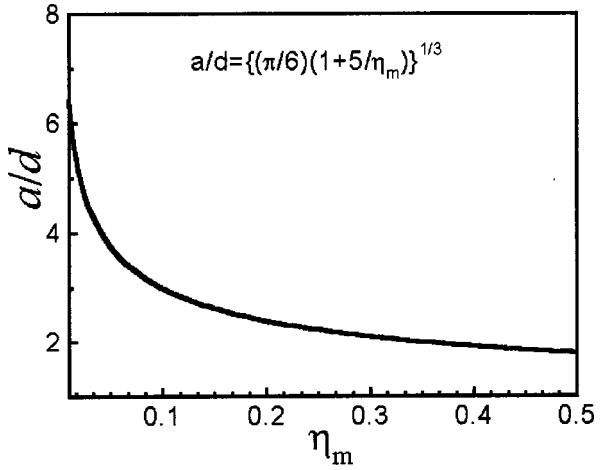

FIG. 9. Calculated concentration dependence of the ratio of the average interparticle distance to the particle diameter in homogeneous NPS.

The dependence in expression (3) on the ratio (a/d) is presented in Fig. 9. The average distance between particles is equal to about $6.4d$ for sample S1 and about $3.8d$ for sample S5. We can anticipate with a fair degree of assurance that the nanoparticles are interacting weakly in both samples.[34]

The EPR spectra observed in our samples contain resonance lines of two types: relatively narrow ($\Delta H_{pp} \approx 100$ Oe at 300 K) signals dominating at high temperatures and broad ($\Delta H_{pp} > 500$ Oe at 300 K) lines prevailing at low temperatures. Traditionally,[12] narrow and broad EPR signals in NPS are attributed to superparamagnetic and ferromagnetic resonance, respectively. The theory of ferromagnetic resonance in bulk materials is relatively well developed.[30] Its results can be summarized as follows.[24] The resonance field H_R of a sample magnetized to saturation by a strong external field is a function of the g factor, of the magnetocrystalline anisotropy field H_A, and the demagnetization field H_S. The anisotropy field may be expressed by $H_A = |K|/M$, where K is the anisotropy constant and M is the sample magnetization. The demagnetization field depends on the shape of the sample. If the sample has the shape of an ellipsoid of rotation around the direction of the applied field, the demagnetization field may be expressed as $H_S = -\Delta N M$, where ΔN is called the anisotropy form factor and is a function of the sample dimensions. ΔN is positive for an oblate ellipsoid and negative for a prolate ellipsoid of rotation for a sphere $\Delta N = 0$. For the resonance field the following relation holds:

$$h\nu/g\beta = H_R + \alpha H_A + H_S, \tag{4}$$

where $h\nu/g\beta$ is a constant equal to the resonance field in the paramagnetic limit, and α is a factor that depends only on the angles between the applied field and the crystal-graphic axes. The latter relation can be written as $H_R = h\nu/g\beta - \alpha|K|/M + \Delta N M$. So, the magnetization of the sample moves the value of H_R from the value for the same sample in the paramagnetic state (above the Curie temperature).

To apply this model, developed for bulk materials, to the nanoparticle system the following assumptions are usually made.[24–26] The system under study is considered to be a coherent assembly of small noninteracting particles embedded in a diamagnetic matrix. All particles have the same intrinsic moment I_S, the same volume V, and the same anisotropy constant K. The applied field H must be strong enough to cause the relation $H \cdot I_S \gg |K|$ (or $H \gg H_A$) to be true. The particles have the shape of an ellipsoid of rotation and the applied field lies along one of the principal axes of the ellipsoid.

Under these conditions, in the case of nanoparticles with an axial magnetic anisotropy, the relation for the resonance field can be expressed as $H_R = h\nu/g\beta - \alpha(|K|/M)(1-2/x) + \Delta N L(x)$, where $x = VHI_S/kT$ and $L(x)$ is the Langevin function.[24] At high temperatures ($x \ll 1$) the anisotropy and demagnetization fields for nanoparticle systems tend to zero. In this case the narrow EPR signal is observed at $H_R \approx h\nu/g\beta$. This is the so-called superparamagnetic resonance.[12] At low temperatures H_A and H_S tend to have their bulk values and the broad signal of the ferromagnetic resonance should be observed.

A superparamagnetic EPR signal was found in magnetite[12] (Fe_3O_4) and maghemite[16–18] (γ-Fe_2O_3) nanoparticles. Some EPR experiments on Fe-based NPS demonstrated only one broad absorption line.[13,15] The lack of a narrow resonance could be due to the rather large size of the particles.[17] Estimations[12,35] show that the average particle diameter would be around 2.6 nm for a linewidth of 170 Oe. Our data demonstrate that increasing the iron concentration in the sample promotes the growth of larger particles.[36] It is important that the superparamagnetic signal disappears in the samples with high iron content (>20 wt %), in which the particle diameter reaches about 4 nm.[36]

Patel *et al.*[13] have assumed that the narrow signal primarily reported by Sharma and Waldner[12] must refer to a resonance from free radicals, which would indicate insufficient purity of the samples. The nonparamagnetic thermal behavior of the narrow signal (Figs. 4 and 7) completely rejects this possibility in the case of our samples.

A general analytical solution to the problem of thermal behavior of superparamagnetic resonance does not yet exist. Numerical results for some important situations were obtained by Raikher and Stepanov.[25,26] They predict that with temperature lowering the shape of the superparamagnetic signal loses its symmetry and becomes powder-pattern-like. On further cooling, only the low-field component of the EPR spectrum remains. Although the finite size distribution and complex nanoparticle composition have not been taken into consideration, these results[25,26] could be qualitatively applicable to our EPR data.

It is clear from Figs. 3, 5, 6, and 8 that a decrease in the intensity of the narrow signal takes place synchronously with the growth of the broad resonance, the position of which is shifted to the lower fields. This indicates that both of these signals have a common superparamagnetic origin. At high temperatures weak-interacting nanoparticles should reveal an EPR signal, which is narrowed by a superparamagnetic fluctuation. When cooling, most large particles undergo a transition to the stable state and demonstrate a rather broad resonance signal. For sample S1, where the average particle diameter d_m is about 2 nm, the transformation of EPR spectra from ''narrow'' to ''broad'' happens below about 25 K

(Figs. 3 and 5). Sample S5, containing larger particles ($d_m = 3.6\,\text{nm}$), displays an analogous spectrum transformation below about 70 K. According to the results of magnetic measurements[36] the ZFC magnetization has a maximum at about 16 K for sample S5 and below 4 K for sample S1 (in the field of 800 Oe). Probably, the temperature–anisotropy parameter $\sigma = KV/k_BT$, which determines the characteristic temperatures for superparamagnetic resonance,[24–26] increases in sample S5 by comparison to sample S1. In general, our EPR data show the temperature-driven transition from superparamagnetic to ferromagnetic resonance in nanoparticles.

An intriguing feature of the superparamagnetic resonance signal is a small shoulder at about 1700 Oe$\approx H_e/2$ (Figs. 3 and 6). This shoulder is a common finding in nanoparticles when the narrow signal is detected.[12,18] Sharma and Waldner[12] attributed this satellite line to a ferromagnetic resonance line shape peculiarity. However, our experiments have shown a weak temperature dependence of this small signal in contrast to the dominant resonance line, call this hypothesis into question. The origin of the ''half-field anomaly'' remains obscure.

Another interesting result of the presented work consists of the observation of an EPR anomaly at about 25 K, both in S1 (Fig. 5) and S5 (Fig. 8). The marked line broadening and decrease of the signal amplitude (Figs. 4 and 7) could be evidence for the complicated magnetic structure of γ-Fe_2O_3 nanoparticles. The internal magnetic structure (''ground state'') of nanoparticles is a subject of great interest.[37] Many experiments point to the existence in γ-Fe_2O_3 nanoparticles of a surface layer which undergoes a spin-glass-like transition near 50 K.[37–40] Martínez *et al.*[38] found that the exchange anisotropy field[41] H_E, which should be considered a component of H_A in Eq. (4), starts increasing below $T_{\text{crit}} = 25\,\text{K}$. The rapid growth of H_E below T_{crit} could result in a significant broadening of the EPR line near 25 K and especially at lower temperatures (Figs. 3 and 6).

V. CONCLUSIONS

Superparamagnetic resonance was observed in samples consisting of Fe-based nanoparticles embedded in a polyethylene matrix. The relatively narrow line of the superparamagnetic resonance, observed at room temperature, is transformed at low temperatures to a broad ferromagnetic resonance signal. The characteristic temperatures of the EPR spectrum changes correlate with the blocking temperatures determined in magnetization measurements, as well as with particle size distributions. The broadening of the EPR linewidth near 25 K may be evidence of the increase of exchange anisotropy field in the spin-glass state which is assumed to exist in iron oxide nanoparticles below 50 K.

ACKNOWLEDGMENTS

The authors are grateful to L. Ponomarenko and M. Mikheev for useful discussions.

[1] J. L. Dormann, E. Tronc, and D. Fiorani, *Advances in Chemical Physics Series* (Wiley, New York, 1997), Vol. 98, Chap. 4, pp. 283–494.
[2] *Magnetic Properties of Fine Particles*, edited by J. L. Dormann and D. Fiorani (North-Holland, Amsterdam, 1992).
[3] I. S. Jacobs and C. P. Bean, in *Magnetism*, edited by G. T. Rado and H. Suhl (Academic, New York, 1963), Vol. 3, p. 271.
[4] S. Mørup, F. Bødker, P. V. Hendriksen, and S. Linderoth, Phys. Rev. B **52**, 287 (1995).
[5] S. Mørup, Europhys. Lett. **28**, 671 (1994).
[6] C. L. Chen, J. Appl. Phys. **69**, 5267 (1991).
[7] B. Elschner and A. Loidl, in *Handbook on the Physics and Chemistry of Rare Earths*, edited by K. A. Gschneider, Jr. and L. Eyring (Elsevier, North-Holland, 1997), Vol. 24, Chap. 162, p. 221.
[8] R. H. Taylor, Adv. Phys. **24**, 681 (1975).
[9] D. M. S. Bagguley, Proc. R. Soc. London, Ser. A **228**, 549 (1955).
[10] Yu. I. Petrov, B. A. Rusin, and Yu. A. Fedorov, Fiz. Met. Metalloved. **23**, 504 (1967).
[11] G. A. Petrakovskii, V. P. Piskorskii, V. M. Sosnin, and I. D. Kosobudskii, Fiz. Tverd. Tela (Leningrad) **25**, 3256 (1983).
[12] V. K. Sharma and F. Waldner, J. Appl. Phys. **48**, 4298 (1977).
[13] J. M. Patel, S. P. Vaidya, and R. V. Mehta, J. Magn. Magn. Mater. **65**, 273 (1987).
[14] U. Netzelman, J. Appl. Phys. **68**, 1800 (1990).
[15] M. M. Ibrahim, G. Edwards, M. S. Seehra, B. Ganguly, and G. P. Huffman, J. Appl. Phys. **75**, 5873 (1994).
[16] F. Gazeau, J. C. Bacri, F. Gendron, R. Perzynski, Yu. L. Raikher, V. I. Stepanov, and E. Dubois, J. Magn. Magn. Mater. **186**, 175 (1998).
[17] F. Gazeau, V. Shilov, J. C. Bacri, E. Dubois, F. Gendron, R. Perzynski, Yu. L. Raikher, and V. I. Stepanov, J. Magn. Magn. Mater. **202**, 535 (1999).
[18] J. W. M. Bulte, R. A. Brooks, B. M. Moskowitz, L. H. Bryant, Jr., and J. A. Frank, J. Magn. Magn. Mater. **194**, 217 (1999).
[19] M. Respaud, M. Goiran, J. M. Broto, F. H. Yang, T. Ould Ely, C. Amiens, and B. Chaudret, Phys. Rev. B **59**, R3934 (1999).
[20] D. L. Griscom, E. J. Friebele, and D. B. Shinn, J. Appl. Phys. **50**, 2402 (1979).
[21] D. L. Griscom, IEEE Trans. Magn. **MAG-17**, 2718 (1981).
[22] K. A. Hempel and W. Roos, IEEE Trans. Magn. **MAG-17**, 2642 (1981).
[23] R. S. Gekht, V. A. Ignatchenko, Yu. A. Raikher, and M. I. Shliomis, J. Exp. Theor. Phys. **70**, 1300 (1976).
[24] R. S. de Biasi and T. C. Devezas, J. Appl. Phys. **49**, 2466 (1977).
[25] Yu. L. Raikher and V. I. Stepanov, Phys. Rev. B **50**, 6250 (1994).
[26] Yu. L. Raikher and V. I. Stepanov, J. Magn. Magn. Mater. **149**, 34 (1995).
[27] F. Gazeau, V. P. Shilov, J.-C. Bacri, E. Dubois, F. Gendron, R. Perzynski, Yu. L. Raikher, and V. I. Stepanov, J. Magn. Magn. Mater. **202**, 535 (1999).
[28] R. W. Chantrell, J. Popplewell, and S. W. Charles, IEEE Trans. Magn. **MAG-14**, 975 (1978).
[29] K. O'Grady and A. Bradbury, J. Magn. Magn. Mater. **39**, 91 (1983).
[30] *Ferromagnetic Resonance*, edited by S. V. Vonsovskii (Pergamon, Oxford, 1966).
[31] B. H. Sohn, R. E. Cohen, and G. C. Papaefthymiou, J. Magn. Magn. Mater. **182**, 216 (1998).
[32] S. Mørup, F. Bødker, P. V. Hendriksen, and S. Linderoth, Phys. Rev. B **52**, 287 (1995).
[33] J. L. Dormann *et al.*, J. Magn. Magn. Mater. **187**, L139 (1998).
[34] J. L. Dormann, F. D'Orazio, F. Lucari, E. Tronc, P. Prene, J. P. Jolivet, D. Fiorani, R. Cherkaoui, and M. Noguès, Phys. Rev. B **53**, 14291 (1996).
[35] S. M. Aharoni and M. H. Litt, J. Appl. Phys. **42**, 352 (1971).
[36] L. Ponomarenko, M. Mikheev, Yu. A. Koksharov, S. P. Gubin, and A. M. Tishin (unpublished).
[37] R. H. Kodama and A. E. Berkowitz, Phys. Rev. B **59**, 6321 (1999).
[38] B. Martínez, X. Obradors, L. Balcells, A. Rouanet, and C. Monty, Phys. Rev. Lett. **80**, 181 (1998).
[39] B. Martínez, A. Roig, E. Molins, T. Gonzalez-Carreño, and C. J. Serna, J. Appl. Phys. **83**, 3256 (1998).
[40] L. Del Bianco, A. Hernando, M. Multigner, C. Prados, J. C. Sánchez-López, A. Fernández, C. F. Conde, and A. Conde, J. Appl. Phys. **84**, 2189 (1998).
[41] A. P. Malozemoff, J. Appl. Phys. **63**, 3874 (1988).